J Am Oil Chem Soc (2012) 89:2245–2252
DOI 10.1007/s11746-012-2119-6

ORIGINAL PAPER

Selective Hydrogenation of Soybean Oil on Copper Catalysts as a Tool Towards Improved Bioproducts

A. F. Trasarti · D. J. Segobia · C. R. Apesteguía · F. Santoro · F. Zaccheria · N. Ravasio

Received: 28 March 2012 / Revised: 17 June 2012 / Accepted: 9 July 2012 / Published online: 1 August 2012

Abstract The liquid-phase soybean oil hydrogenation was studied on silica-supported Cu and ternary Cu–Zn–Al catalysts. Cu/SiO_2 samples were prepared by incipient-wetness impregnation (Cu/SiO_2-Imp) and chemisorption-hydrolysis (Cu/SiO_2-CH), while two Cu–Zn–Al mixed oxides containing 8 (Cu(8)–Zn–Al) and 15 % Cu (Cu(15)–Zn–Al), respectively, were prepared by coprecipitation. Copper dispersion (D_{Cu}) was 23 % on Cu/SiO_2-CH, and this sample showed a high activity for soybean oil hydrogenation; in contrast, Cu/SiO_2-Imp was inactive, probably because Cu was poorly dispersed ($D_{Cu} = 2$ %). The oil hydrogenation activity on Cu(15)–Zn–Al ($D_{Cu} = 9$ %) was lower than on Cu/SiO_2-CH, while Cu(8)–Zn–Al ($D_{Cu} = 23$ %) was inactive. Citral hydrogenation used as a test reaction showed that the intrinsic Cu^0 activity was not significantly changed by the kind of support or the catalyst preparation method. These latter results suggested that the observed differences in soybean oil hydrogenation may be explained as changes in accessibility of the triglyceride molecules to Cu active sites. In ternary Cu–Zn–Al samples, access to catalytic sites was hampered by the narrower pore structure of the catalyst. Copper exhibited unique properties for obtaining proper lubricants from soybean oil hydrogenation because selectively hydrogenated unsaturated linolenic (C18:3) and linoleic (C18:2) fatty acids to unsaturated oleic acid (C18:1) without forming saturated stearic acid (C18:0).

Keywords Soybean oil · Citral · Cu catalysts · Selective hydrogenation

A. F. Trasarti (✉) · D. J. Segobia · C. R. Apesteguía
Catalysis Science and Engineering Research Group (GICIC), INCAPE (UNL-CONICET), Santiago del Estero 2654, 3000 Santa Fe, Argentina
e-mail: trasarti@fiq.unl.edu.ar
URL: http://www.fiq.unl.edu.ar/gicic

F. Santoro · F. Zaccheria · N. Ravasio
CNR-Istituto di Scienze e Tecnologie Molecolari, via C. Golgi 19, 20133 Milan, Italy

Introduction

Solid catalysts are often used in organic synthesis for the hydrogenation of functional groups. In particular, the selective hydrogenation of complex substrates to obtain fine chemicals has been largely investigated on noble metal-based catalysts (Pt, Pd, Rh) [1]. In the last decades, the development of optimized catalyst formulations using less expensive non-noble metals (Ni, Co, Cu) resulted in new highly selective processes for hydrogenation reactions, including the valorization of biomass raw materials [2]. Among these, vegetable oils certainly represent an important bioresource, providing interesting products for a wide variety of chemical divisions, albeit their profitable application strongly depends on availability and supply. Production of soybean oil has continuously grown up in the last years, reaching more than 38 million tons in 2010, of which 7.5 million tons come from Argentina [3]. Moreover, strong efforts have been made to minimize the energy inputs in the soy cultivation step. Although the biodiesel market represents the main destination of soybean oil in Argentine, the synthesis of more valuable chemical products from it represents certainly an attractive technological and economical strategy.

The hydrogenation of vegetable oils using Ni-based catalysts to produce margarines and spreadables is a well-known industrial process. However, the reaction is not selective and keeps going until full saturation of the fatty

acid chain is reached, converting the oil to a solid material. In the last few years, increasing research efforts have been focused on the development of new oil hydrogenation catalysts to obtain oils with improved oxidative stability to be used as oleochemistry feedstocks, e.g., for the production of environmentally friendly, biodegradable lubricants. Vegetable oils possess superior tribological properties such as good contact lubrication, an elevated flash point, a high viscosity index and low volatility [4]. Nevertheless, plant oils suffer from poor low temperature fluidity and have a higher sensitivity to hydrolysis and oxidative attacks as compared to mineral oils. Chemical modifications of vegetable oils can overcome these shortcomings [5]; for example, the oxidation stability is improved by hydrogenating the double bond functionality. The main unsaturated fatty acids in soybean oil are linolenic (C18:3), linoleic (C18:2) and oleic (C18:1). Their oxygen absorption rate is respectively 100:40:1 [6]. Thus, partial hydrogenation of C18:3 and C18:2 to C18:1 (Fig. 1) strongly increases the soybean oil stabilization towards oxygen. However, unsaturated C18:1 fatty acid should not be hydrogenated to stearic acid (C18:0) in order not to increase significantly the pour point, which also depends on the *cis/trans* isomers ratio because of the higher melting point of the *trans*-isomer. Copper-based catalysts have been used in edible oil hydrogenation because they promote the selective reduction of C18:3 to C18:1, leaving linoleate C18:2 unaffected, a valuable component from the nutritional point of view [7]. Recently, some of us [8] reported that pre-reduced Cu supported on silica exhibits unusual activity in the hydrogenation of different fatty acid methyl esters, with strong stabilization of the product towards oxidation, while also keeping cold properties for their use as biodiesel.

Here, we study the liquid-phase hydrogenation of soybean oil on different Cu-supported catalysts. Specifically, we prepared two Cu/SiO_2 catalysts either by impregnation or chemisorption-hydrolysis methods, and two ternary

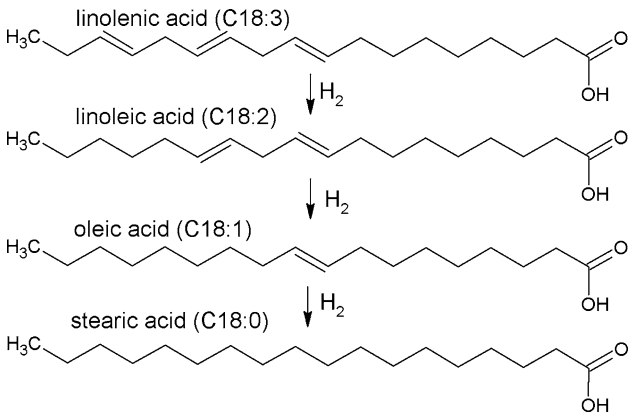

Fig. 1 Selective hydrogenation of linolenic acid

Cu–Zn–Al samples by coprecipitation. The objective was to establish the effect of sample properties (Cu dispersion, surface area and porous structure of supports) and reactant size on the catalyst activity and selectivity.

Experimental

Catalyst Preparation

Two silica-supported Cu catalysts were prepared. A Cu/SiO_2-Imp sample was obtained by incipient-wetness impregnation using aqueous Cu nitrate solutions ($Cu(NO_3)_2{\cdot}6H_2O$, Fluka 98 %) and a commercial silica (Davidson G62, 99.7 %). The impregnated sample was first dried overnight at 363 K and then calcined in air (60 cm^3/min) at 623 K for 4 h. Cu/SiO_2-CH was prepared by the chemisorption-hydrolysis method as reported previously [9], by adding the support (Grace Davison Davisil grade 634) to a solution containing $[Cu(NH_3)_4]^{2+}$ and slowly diluting the slurry with water. The solids were separated by filtration, washed with water, dried overnight at 383 K and calcined in air at 623 K for 4 h.

Hydrated precursors of ternary Cu–Zn–Al mixed oxides were prepared by coprecipitation as described elsewhere [10, 11]. An acidic solution of the metal nitrates (Aldrich 98 %) was contacted with an aqueous solution of K_2CO_3 at a constant pH of 7. The two solutions were simultaneously added dropwise to 400 mL of distilled water kept at 338 K in a stirred batch reactor. The resulting precipitates were aged for 2 h in their mother liquor and then filtered, washed thoroughly with deionized water at 338 K and finally dried at 363 K overnight. Dried precipitates were decomposed in nitrogen at 673 K for 8 h in order to obtain the corresponding mixed oxides. Two samples with nominal Cu loadings of 8 and 15 % were prepared and are identified here as Cu(8)–Zn–Al and Cu(15)–Zn–Al samples, respectively.

Catalyst Characterization

Surface areas (S_g) and pore size distribution of the samples were measured by N_2 physisorption at 77 K using the BET method and Barret-Joyner-Halender (BJH) calculations, respectively, in a Quantochrome NOVA-1000 sorptometer; total pore volumes were also measured during the analysis. Before adsorption, the samples were treated at 623 K under vacuum for 8 h. Copper content was determined by atomic absorption spectroscopy (AAS).

The crystal structure of the samples was determined by powder X-ray diffraction (XRD) methods using a Shimadzu XD-D1 diffractometer and Ni-filtered CuKa radiation. The diffraction patterns were scanned in the 2θ of 10–80°.

The mean crystallite sizes of Cu^0 and CuO were determined by using the Debye-Scherrer equation.

The metallic copper dispersions (D_{Cu} = surface Cu atoms/total Cu atoms) were measured by titration with N_2O at 363 K using a stoichiometry of $(Cu^0)_s/N_2O = 2$, where $(Cu^0)_s$ implies copper atom on surface [12]. Pre-reduced samples were exposed to pulses of N_2O in a flow of He. The number of chemisorbed oxygen atoms was calculated from the consumption of N_2O measured by mass spectrometry in a Balzers Omnistar spectrometer. The mean Cu^0 crystallite size was calculated by assuming an fcc structure and a surface density of 1.35×10^{19} Cu atoms/m^2 [13].

Temperature-programmed reduction (TPR) experiments were performed using a 5 % H_2/Ar mixture (50 mL/min) in a Micromeritics AutoChem II 2920 unit equipped with a thermal conductivity detector (TCD). Calcined samples (150 mg) were heated at 10 K/min from 298 to 1,123 K. In order to retain water formed during sample reduction, the exit gas from the reactor was passed through a cold trap before entering the TCD detector.

Catalytic Tests

The hydrogenation of soybean oil was carried out at conditions near those of a standard industrial process for this reaction [14], i.e., 453 K, 1,000 rpm and 2.2 MPa (H_2) in a 60-mL SS AISI 316 autoclave equipped with a stirring rod, magnetic stirring head, digital pressure display and a sampling device. Catalysts (0.8 g) were outgassed in vacuum at 543 K for 20 min and then reduced with H_2 at the same temperature while carefully removing the water formed under vacuum, and finally transferred to the reactor together with the oil (40 mL) in an inert atmosphere. Reaction mixtures were analyzed on an Agilent 6850 GC equipped with an FID detector using a 100-m SP2560 column of 250-μm diameter. Samples were periodically withdrawn from the reactor and transesterified with a 2 N solution of KOH in methanol previously to the analysis by gas chromatography. The soybean oil triglyceride composition was: 10.9 % C16:0, 3.7 % C18:0, 24.9 % C18:1, 52.7 % C18:2 and 4.8 % C18:3 (where the first number denotes the total carbon number of the acyl groups and the second number stands for the total number of double bonds). The initial unsaturation of the soybean oil in terms of the iodine value (IV) was 129.

Physical properties of soybean and hydrogenated oils were determined by different chemical methods. The free fatty acid content (acidity, %wt) was measured by titration with a 0.1 N NaOH solution after dissolving the samples with ethanol/diethylether (1/2). The iodine value (IV) was determined both by calculation on the basis of GC fatty acid composition and by iodine titration. The iodine value expresses the degree of unsaturation of the oil as: IV = g of iodine absorbed/100 g of oil. Pour points were measured by pouring the sample into a test jar provided with a thermometer. The sample was first cooled to solidification and then slowly heated in a water bath to register the pour point.

The liquid-phase hydrogenation of citral (Aldrich, 98 %) was studied in a Parr 4843 reactor at 393 K, using isopropanol (Cicarelli, p.a.) as solvent. The autoclave was loaded with 150 mL of solvent, 1 mL of citral, 0.5 g of catalyst and 0.5 mL of octanol as internal standard. Prior to catalytic tests, samples were reduced ex-situ in hydrogen (30 mL/min) for 2 h at 543 K and loaded immediately to the reactor under inert atmosphere. The reaction system was heated to the reaction temperature at 2 K/min, and the pressure was then rapidly increased to 1,013 kPa with H_2. Product concentrations were followed during the reaction by ex-situ gas chromatography using an Agilent 6850 GC chromatograph equipped with a flame ionization detector, temperature programmer and a 30-m Supelco α-DEX capillary column. Samples from the reaction system were taken by using a loop under pressure in order to avoid flushing. Data were collected every 15–30 min for 300–500 min. Conversion of citral was calculated as $X_{Cit} = (C^0_{Cit} - C_{Cit})/C^0_{Cit}$, where C^0_{Cit} is the initial concentration of citral and C_{Cit} is the concentration of citral at reaction time t. Selectivities (S_j, mol of product j/mol of citral reacted) were calculated as S_j (%) $= C_j \times 100/\Sigma C_j$ where C_j is the concentration of product j. Yields (η_j, mol of product j/mol of citral fed) were calculated as $\eta_j = S_j\, X_{Cit}$.

Results and Discussion

Catalyst Characterization

The physicochemical properties of the catalysts used in this work are summarized in Table 1. The Cu loading on the four samples was between 7.7 and 15.0 %. The crystalline CuO phase was detected by X-ray diffraction only on Cu/SiO_2-Imp (Fig. 2), suggesting that copper was well dispersed on the other three samples. The CuO crystallite size in the Cu/SiO_2-Imp sample determined from the corresponding diffractogram in Fig. 2 was 20 nm. XRD patterns of Cu–Zn–Al hydrated precursors (not shown here) exhibited a single crystalline phase with hydrotalcite structure (ASTM 14-191) consisting of layered double hydroxides with brucite-like layers and $[(\Sigma Me^{2+})_{1-x} Al_x(OH)_2]^{x+}(CO_3)^{2-}_{x/2}.mH_2O$ composition, where Me is Cu or Zn. Thermal decomposition of hydrotalcite precursors leads to the formation of very small CuO particles in a super-stoichiometric zinc aluminate spinel phase (ASTM

Table 1 Chemical, structural and textural properties of the catalysts used in this work

Catalyst	Cu loading[a] (wt%)	Crystalline phase	Surface area S_g (m^2/g)	Pore volume V_p (cm^3/g)	Pore diameter D_p (Å)	Cu dispersion D_{Cu} (%)	TPR: CuO reduction peak T_{max} (K)
Cu/SiO_2-Imp	9.6	CuO	256	0.90	200	2	541
Cu/SiO_2-CH	11.0	Not detected	388	0.60	80	21	537
Cu(8)–Zn–Al	7.7	Spinel	120	0.15	52	23	518
Cu(15)–Zn–Al	15.0	Spinel	139	0.20	62	9	464

[a] Determined by AAS

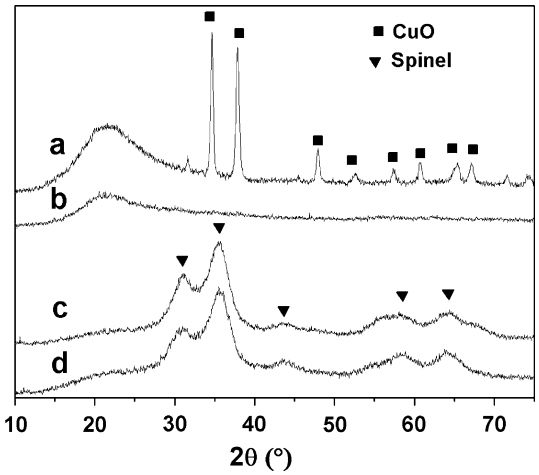

Fig. 2 XRD patterns of the catalysts used in this work; **a** Cu/SiO_2-Imp, **b** Cu/SiO2-CH, **c** Cu(8)–Zn–Al, **d** Cu(15)–Zn–Al

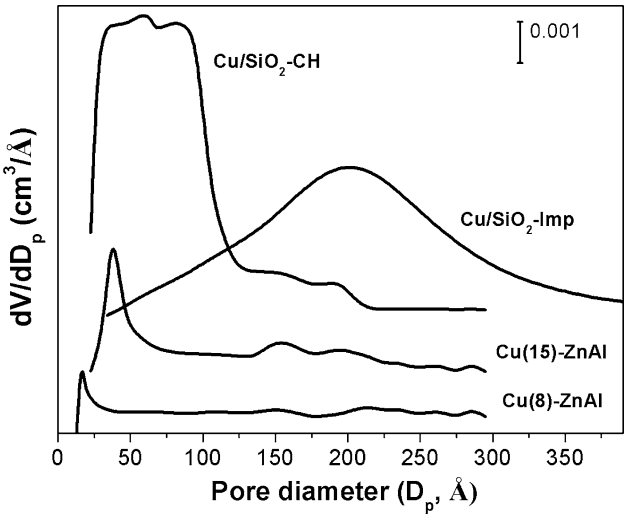

Fig. 3 Pore size distribution of Cu-based samples

Standard 5-0669) [15]. In our case, their general formula, on a spinel-like basis, is approximately $[CuO]_{0.35}[ZnO]_{0.65}ZnAl_2O_4$ (Cu(8)–Zn–Al sample) and $[CuO]_{0.65}[ZnO]_{0.35}ZnAl_2O_4$ (Cu(15)–Zn–Al sample). No segregation of CuO or ZnO crystalline phases of large crystallite size were detected in the Cu–Zn–Al mixed oxides, thereby indicating that both cations are highly dispersed in the spinel-like matrix.

BET surface areas of Cu–Zn–Al mixed oxides were similar, between 120 and 140 m^2/g, and lower than those determined for Cu/SiO_2-Imp (256 m^2/g) and Cu/SiO_2-CH (388 m^2/g, Table 1). Pore size distributions are shown in Fig. 3, and mean pore sizes are included in Table 1. Sample Cu/SiO_2-Imp exhibited a Gaussian-like pore distribution and the largest mean pore size (about 200 Å). Ternary Cu–Zn–Al mixed oxides showed a Gaussian-like pore distribution in the 20–60 Å region, but contained also mesopores between 100 and 300 Å (Fig. 3). The mean pore sizes of Cu–Zn–Al samples were clearly smaller than those of SiO_2-supported samples (Table 1). The metallic Cu dispersion was about 20–25 % on Cu/SiO_2-CH and Cu(8)–Zn–Al, but decreased to 9 % on sample Cu(15)–Zn–Al, probably because of the increase of the mean crystallite size as a consequence of Cu segregation at that higher Cu loading. Thus, Cu segregation should be pointed out as the origin of a slight increase of the mean pore size in Cu(15)–Zn–Al when compared with Cu(8)–Zn–Al (62 and 52 Å, respectively, Table 1; Fig. 3). Copper was poorly dispersed on Cu/SiO_2-Imp ($D_{Cu} = 2$ %), as usually happens with catalysts prepared by the incipient-wetness impregnation method (Table 1).

Figure 4 shows the TPR profiles of Cu/SiO_2 and Cu–Zn–Al samples. Cu/SiO_2 samples exhibited a single low-temperature peak at ca. 540 K (Table 1) arising from the reduction of CuO to metallic copper. TPR traces of Cu(8)–Zn–Al and Cu(15)–Zn–Al also showed the CuO reduction peaks, but the peak maxima were shifted to lower temperatures compared to Cu/SiO_2 samples (Table 1). A broader consumption band in Cu(8)–Zn–Al takes account of differences in reducibility between more segregated CuO crystallites (at lower temperature, ca. 480 K) and those deeply inside the spinel matrix (around 540 K), while in Cu(15)–Zn–Al the more segregated CuO band is bigger and overlaps the other at higher temperature (Fig. 4). Ternary Cu–Zn–Al samples also presented an additional H_2

consumption band at temperatures higher than 700 K, which has been attributed to the partial reduction of ZnO, followed by the formation of brass. Thus, treatment of Cu–Zn–Al samples with diluted H_2/N_2 mixtures at temperatures lower than 700 K only reduces the CuO phase. By integration of the CuO reduction peaks in Fig. 4, we verified that complete reduction of CuO to Cu^0 takes place on all the samples.

Soybean Oil Hydrogenation

The catalyst activity and selectivity for the liquid-phase hydrogenation of refined soybean oil were evaluated through standard 3-h catalytic runs. Figure 5 shows the reactant evolution and product compositions obtained at 453 K on Cu/SiO_2-CH and Cu(15)–Zn–Al samples and typically illustrates the catalyst behavior during the reaction. Results obtained at the end of the runs for all the catalysts are shown in Table 2. The Cu/SiO_2-Imp sample was practically inactive after 24 h reaction. This result is consistent with previous reports showing that low-dispersed Cu/SiO_2 catalysts prepared by incipient wetness did not show any activity for oil hydrogenation even after long reaction times [16]. In contrast, Cu/SiO_2-CH showed a high hydrogenation activity, decreasing the IV value of soybean oil from 129 to 97. In 3 h, Cu/SiO_2-CH almost completely eliminated C18:3 (0.3 %) and decreased the concentration of C18:2 from 52.7 to 31.3 %. As a consequence, the concentration of C18:1 increased from 24.9 to 52.2 % since that of saturated C18:0 fatty acid did not change during the reaction (Fig. 5); neither did the saturated C16:0 concentration. The pour point and acidity of the soybean oil hydrogenated on Cu/SiO_2-CH were not significantly higher than those of starting oil, while the amount of

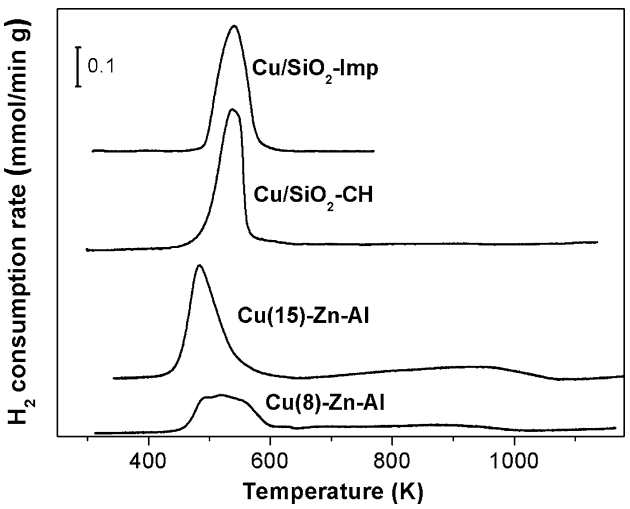

Fig. 4 Sample characterization by TPR. Heating rate 10 K/min, *W* 150 mg

trans-isomers was only 13.8 %. Thus, the results obtained on Cu/SiO_2-CH point out that highly dispersed copper on silica is a very efficient catalyst for selectively hydrogenating C18:3 and C18:2 to monounsaturated C18:1, without producing stearic acid, and confirm that copper is a very efficient metal for obtaining proper lubricants by oil hydrogenation.

Regarding ternary Cu–Zn–Al samples, Cu(8)–Zn–Al was practically inactive, while Cu(15)–Zn–Al showed good hydrogenation activity and selectivity (Table 2; Fig. 5). Specifically, Cu(15)–Zn–Al almost totally hydrogenated C18:3 (0.5 %) and decreased the amount of C18:2 from 52.7 to 41.6 %, thereby increasing the C18:1 concentration from 24.9 to 41.6 %. As observed for Cu/SiO_2-CH, C18:1 was not hydrogenated to C18:0 on Cu(15)–Zn–Al and thus the C18:0 concentration did not change during the catalytic test (Fig. 5). Nevertheless, the activity of Cu(15)–Zn–Al for hydrogenating C18:3 and C18:2 was lower than that of Cu/SiO_2-CH. For example, the IV values of oils hydrogenated on Cu(15)–Zn–Al and Cu/SiO_2-CH were 109 and 97, respectively (Table 2). The fact that Cu(15)–Zn–Al was less active than Cu/SiO_2-CH in spite of containing a higher Cu concentration probably reflects a lower accessibility of unsaturated triglyceride molecules to the Cu active sites in Cu(15)–Zn–Al. Actually, the surface area, pore volume and pore size of Cu(15)–Zn–Al were significantly lower in comparison to Cu/SiO_2-CH (Table 1). In this regard, we determined the sizes of two of the most stable configurations of a triglyceride molecule (glyceryl trioleate) by using CHARMM parametrization-based force field optimization calculus [17]. Triglyceride molecule lengths between 29 and 50 Å were calculated, thereby showing that the mean pore sizes of ternary Cu–Zn–Al samples, especially of Cu(8)–Zn–Al, are close to the kinetic diameter of a triglyceride molecule.

As a tool for determining the presence of differences in the hydrogenating activity of Cu due to the occurrence of the support effect, all catalysts were also tested in citral hydrogenation at 393 K. The purpose was to use a smaller polyunsaturated molecule, with no diffusive restrictions to access to the active sites. This statement is supported by several works from other groups and our experience [18–28]. Figure 6 shows the reaction network for citral hydrogenation, where selectivity essentially depends both on the nature of the metallic catalyst and, eventually, on the support, which determines the relative hydrogenation rate of isolated C=C and conjugated C=O and C=C bonds of the citral molecule [19, 21, 22, 25–27]. The possible hydrogenation products are: geraniol/nerol, citronellal, citronellol, 3,7-dimethyl-octanal (3,7-DMEAL), 3,7-dimethyl-octenal (3,7-DMEL), 3,7-dimethyl-octenol (3,7-DMEOL) and 3,7-dimethyl-octanol (3,7-DMOL) (Fig. 6). It is well known that Cu does not hydrogenate the isolated C=C bond of

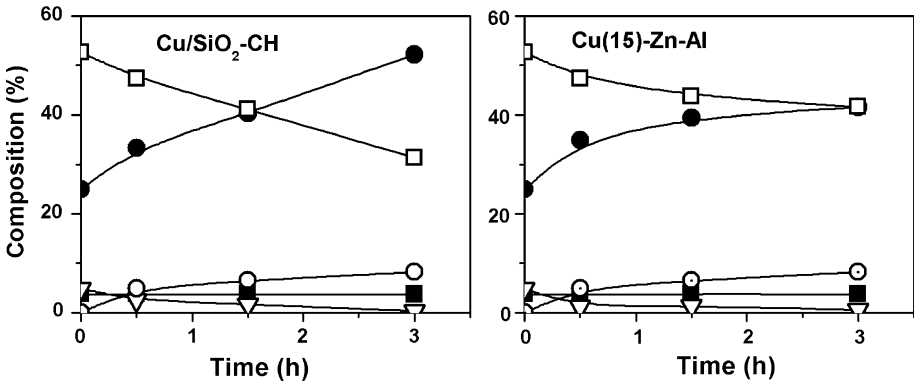

Fig. 5 Soybean hydrogenation. Product composition as a function of time (*filled squares*) C18:0, (*filled circles*) C18:1, (*open squares*) C18:2, (*inverted triangles*) C18:3, (*open circles*) C18:1 trans. [453 K, 2,026 kPa hydrogen, $W = 0.8$ g, $V_{oil} = 40$ mL]

Table 2 Catalytic results for soybean hydrogenation

Catalyst	Time (h)	Fatty acid composition (%)					*Trans*-(%)	Pour point (K)	IV	Acidity (%)
		Palmitic C16:0	Stearic C18:0	Oleic C18:1	Linoleic C18:2	Linolenic C18:3				
		10.9	**3.7**	**24.9**	**52.7**	**4.8**	**0**	248–250	129	0.15
Cu/SiO_2-Imp	24	11.0	3.7	25.0	53.0	4.1	–	–	–	–
Cu/SiO_2-CH	3	11.3	3.7	52.2	31.3	0.3	13.8	266–265	97	0.56
Cu(8)–Zn–Al	3	11.5	4.4	25.4	51.2	4.3	–	–	–	–
Cu(15)–Zn–Al	3	11.1	3.7	41.6	41.6	0.5	8.2	263	109	0.35

$T = 453$ K, $P = 2{,}026$ kPa, $W_{cat} = 0.8$ g, $V_{oil} = 40$ mL

The initial composition of soybean oil is in bold

citral [28]; thus in Fig. 7 the product distribution is shown as a function of time for citral hydrogenation on Cu/SiO_2-Imp, which represents the general behavior of all catalysts tested in this reaction. All the catalysts initially formed citronellal at higher rates in comparison to the formation of geraniol/nerol, thereby indicating that metallic copper hydrogenates preferentially the conjugated C=C bond of citral. Moreover, whereas the geraniol/nerol yield remained almost constant after total conversion of citral, citronellal was consecutively hydrogenated to citronellol (Fig. 7). In summary, the selectivity was not affected by the support or preparation method employed in the set of catalysts. From the initial slopes of X_{Cit} versus t curves like in Fig. 7, the initial citral conversion rates (r^0_{Cit}, mol/g_{Cu} h) were determined for all the catalysts; the results are shown in Table 3. The r^0_{Cit}values followed the order: Cu/SiO_2-CH > Cu(8)–Zn–Al > Cu(15)–Zn–Al $\gg$ Cu/SiO_2-Imp. Nevertheless, when the initial turnover citral conversion rates (TOF, h^{-1}) were determined by using Cu dispersion values of Table 1, we observed that the activity per Cu surface atom was similar on all the catalysts (Table 3). This result suggested that the intrinsic Cu^0 activity for the initial citral hydrogenation is not significantly changed by the kind of support or the catalyst preparation method. Thus, the r^0_{Cit} values on Cu-based catalysts would essentially depend on Cu dispersion: the higher the D_{Cu} is, the higher the r^0_{Cit}.

On the basis of the last discussion, the results in Table 2 showing that Cu(8)–Zn–Al was inactive for oil hydrogenation may be explained by considering that, because of diffusional constraints, the triglyceride molecules do not reach the Cu active sites located in the $ZnAl_2O_4$ porous structure. Other authors [29] have reported that the oil hydrogenation rate is controlled by mass transfer phenomena when performed at operational conditions similar to those employed here. In contrast to Cu(8)–Zn–Al, the ternary Cu(15)–Zn–Al sample was active for oil hydrogenation. Probably, the higher Cu concentration in Cu(15)–Zn–Al favored the formation of more CuO segregated from the $ZnAl_2O_4$ structure, as discussed in "Catalyst Characterization," which would increase the accessibility of reactants to Cu-active sites.

In summary, the results of Fig. 5 and Table 2 show that Cu exhibits unique properties for obtaining proper lubricants from soybean oil hydrogenation, as it is able to enrich the oil in the monounsaturated component without increasing the stearic acid amount, therefore keeping acceptable cold properties. This particular selectivity does not depend on the support (compare Cu/SiO_2-CH with Cu(15)–Zn–Al). Nevertheless, the copper catalyst activity depends on both the Cu dispersion (low-dispersed catalysts are inactive) and the oil accessibility to Cu active sites (supports of wide porous structure are required).

Fig. 6 Reaction network for citral hydrogenation

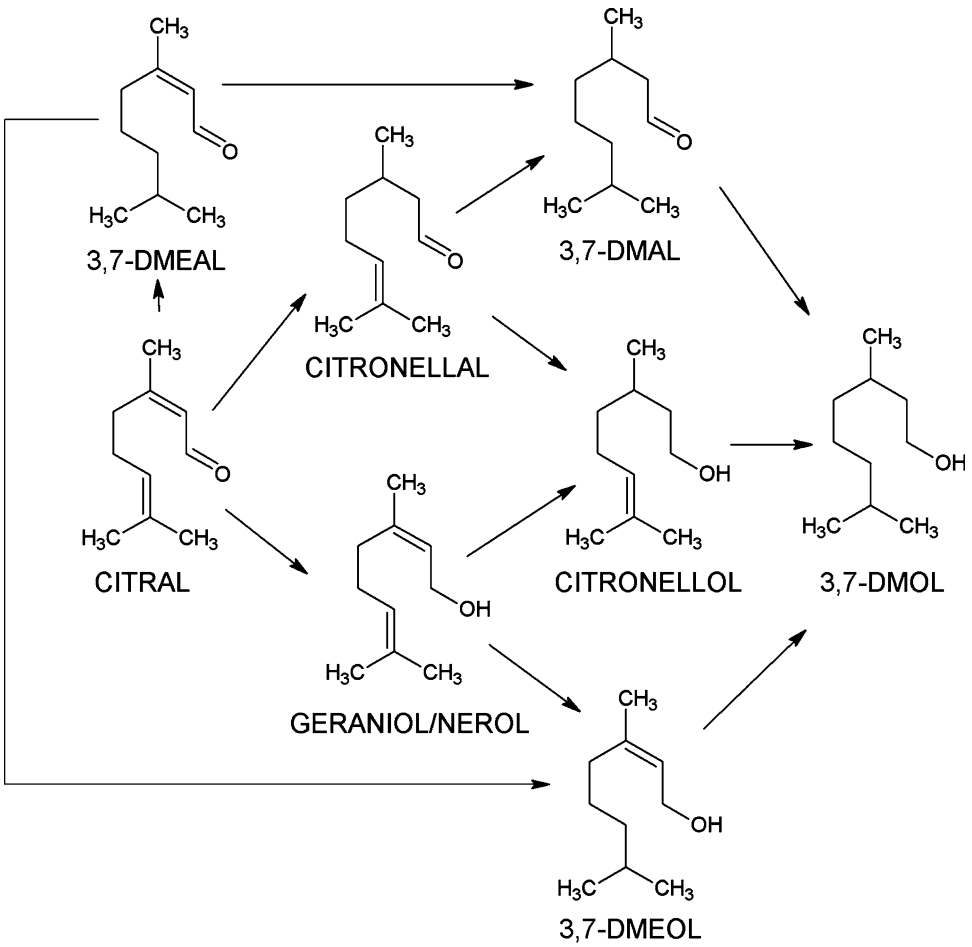

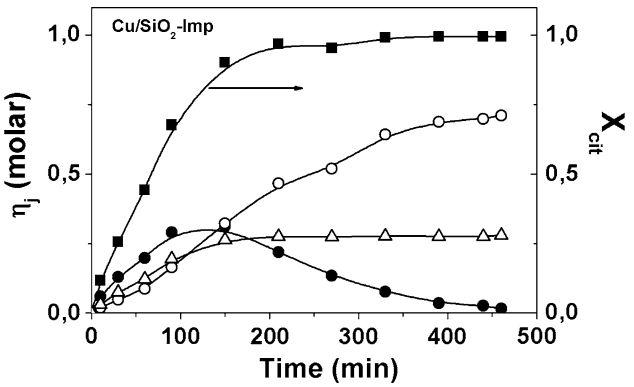

Fig. 7 Citral hydrogenation. Yields (h_j) and citral conversion (X_{cit}) as a function of time for hydrogenation performed over Cu/SiO_2-Imp catalyst. (*open triangles*) geraniol/nerol, (*filled circles*) citronellal, (*open circles*) citronellol. [393 K, 1,013 kPa hydrogen, $W = 0.5$ g]

Table 3 Catalytic results for citral hydrogenation

Catalyst	Initial citral hydrogenation rate	
	r^0_{Cit} (mol/g_{Cu} h)	TOF (h^{-1})
Cu/SiO_2-Imp	0.06	190
Cu/SiO_2-CH	0.54	164
Cu(8)–Zn–Al	0.47	130
Cu(15)–Zn–Al	0.26	183

T = 393 K, P = 1013 kPa, W_{cat} = 0.5 g, citral:toluene = 1:150 (mL)

The use of nontoxic copper systems represents a valuable and versatile tool in order to upgrade different kind of starting materials, both vegetable oils and terpenic substrates. Among terpenes citral, which is the main component (75–90 % of total) of *lemongrass* oil, constitutes a precious raw material that can be transformed into value-added products. On the other hand the transformation of vegetable oils, due to the particular nature of triglycerides, requires more specific solutions—which can be conveniently achieved by varying the materials used as the support for the active metallic phase.

Conclusions

Cu-supported catalysts efficiently promote liquid-phase soybean oil hydrogenation. However, the catalyst activity

and selectivity depend on the copper dispersion and the porous structure of the support.

Copper catalysts selectively hydrogenate unsaturated linolenic (C18:3) and linoleic (C18:2) fatty acids to unsaturated oleic acid (C18:1) without forming saturated stearic (C18:0) acid. However, highly active Cu-based catalysts for soybean oil hydrogenation are obtained only if copper is highly dispersed on supports of wide pore structure for minimizing mass-transfer limitations.

Acknowledgments This work was undertaken in the framework of the cooperation program between CONICET (Concejo Nacional de Investigaciones Científicas y Técnicas, Argentina) and CNR (Consiglio Nazionale delle Ricerche, Italy).

References

1. Augustine RL (1996) Heterogeneous catalysis for the synthetic chemist. Marcel Dekker Inc., New York
2. Climent MJ, Corma A, Iborra S (2011) Heterogeneous catalysts for the one-pot synthesis of chemicals and fine chemicals. Chem Rev 111:1072–1133
3. Gunstone FD (2012). Oils and fat in the market place. Commodity oils and fats. Soybean Oil. The AOCS Lipid Library. http://lipidlibrary.aocs.org/market/soybean.htm. Accessed Jan
4. Boyde S (2002) Green lubricants. Environmental benefits and impacts of lubrication. Green Chem 4:293–307
5. Wagner H, Luther R, Mang T (2001) Lubricant base fluids based on renewable raw materials: their catalytic manufacture and modification. Appl Catal A Gen 221:429–442
6. Frankel EN (2005) Lipid Oxidation, 2nd edn. The Oily Press, Bridgewater
7. Johansson LE (1980) Copper catalysts in the selective hydrogenation of soybean and rapeseed oils: IV. Copper on silica gel, phase composition and preparation. J Am Oil Chem Soc 57:16–22
8. Zaccheria F, Psaro R, Ravasio N (2009) Selective Oil hydrogenation of alternative oils: a useful tool for the production of biofuels. Green Chem 11:462–465
9. Boccuzzi F, Martra G, Coluccia S, Ravasio N (1999) Cu/SiO_2 and Cu/SiO_2–TiO_2 catalysts: I. TEM, DR UV–Vis–NIR, and FTIR Characterisation. J Catal 184:316–326
10. Ginés MJL, Marchi AJ, Apesteguía CR (1997) Kinetic study of the reverse water-gas shift reaction over $CuO/ZnO/Al_2O_3$ catalysts. Appl Catal A Gen 154:155–171
11. Marchi AJ, Gordo DA, Trasarti AF, Apesteguía CR (2003) Liquid phase hydrogenation of cinnamaldehyde on Cu-based catalysts. Appl Catal A Gen 249:53–67
12. Dandekar A, Vannice MA (1998) Determination of the dispersion and surface oxidation states of supported Cu catalysts. J Catal 178:621–639
13. Osinga ThJ, Linsen EG, van Beet WP (1967) The determination of the specific copper surface area in catalysts. J Catal 7:277–279
14. Piqueras CM, Tonetto G, Bottini S, Damiani DE (2008) Sunflower oil hydrogenation on Pt catalysts: Comparison between conventional process and homogeneous phase operation using supercritical propane. Catal Today 133-135:836–841
15. Marchi AJ, Apesteguía CR (1998) Impregnation-induced memory effect of thermally activated layered double hydroxides. Appl Clay Sci 13:35–48
16. Zaccheria F, Psaro R, Ravasio N, Bondioli P (2012) Standarization of vegetable oil composition to be used as oleochemistry feedstock through a selective hydrogenation process. Eur J Lipid Sci Tech 114:24–30
17. Brooks BR, Bruccoleri RE, Olafson BD, States DJ, Swaminathan S, Karplus M (1983) CHARMM: a program for macromolecular energy, minimization, and dynamics calculations. J Comput Chem 4:187–217
18. Álvarez-Rodríguez J, Rodríguez-Ramos I, Guerrero-Ruiz A, Arcoya A (2011) Selective hydrogenation of citral over Pt/KL type catalysts doped with Sr, La, Nd and Sm. Appl Catal A Gen 401:56–64
19. Aramendía MA, Borau V, Jiménez C, Marinas JM, Porras A, Urbano FJ (1997) Selective liquid-phase hydrogenation of citral over supported palladium. J Catal 172:46–54
20. Galvagno S, Milone C, Donato A, Neri G, Pietropaolo R (1993) Hydrogenation of citral over Ru-Sn/C. Catal Lett 17:55–61
21. Lafaye G, Ekou T, Micheaud-Especel C, Montassier C, Marecot P (2004) Citral hydrogenation over alumina supported Rh-Ge catalysts: effects of the reduction temperature. Appl Catal A Gen 257:107–117
22. Mäki-Arvela P, Tiainen LP, Lindblad M, Demirkan K, Kumar N, Sjöholm R, Ollonqvist T, Väyrynen J, Salmi T, Murzin DYu (2002) Liquid-phase hydrogenation of citral for production of citronellol: catalyst selection. Appl Catal A Gen 241:271–288
23. Mäki-Arvela P, Kumar N, Kubicka D, Nasir A, Heikkilä T, Lehto VP, Sjöholm R, Salmi T, Murzin TYu (2005) One-pot citral transformation to menthol over bifunctional micro- and mesoporous metal modified catalysts: effect of catalyst support and metal. J Mol Catal A Chem 240:72–81
24. Recchia S, Dossi C, Poli N, Fussi A, Sordelli L, Psaro R (1999) Outstanding performances of magnesia-supported platinum–tin catalysts for citral selective hydrogenation. J Catal 184:1–4
25. Reyes P, Rojas H, Pecchi G, Fierro JLG (2002) Liquid-phase hydrogenation of citral over Ir-supported catalysts. J Mol Catal A Chem 179:293–299
26. Singh UK, Vannice MA (2001) Liquid-phase citral hydrogenation over SiO_2—supported group VIII metals. J Catal 199:73–84
27. Trasarti AF, Marchi AJ, Apesteguía CR (2004) Highly selective synthesis of menthols from citral in a one-step process. J Catal 224:484–488
28. Trasarti AF, Marchi AJ, Apesteguía CR (2007) Design of catalyst systems for the one-pot synthesis of menthols from citral. J Catal 247:155–165
29. Fernández MB, Piqueras CM, Tonetto GM, Crapiste GH, Damiani DE (2005) Hydrogenation of edible oil over $Pd\text{-}Me/Al_2O_3$ catalysts (Me = Mo, V and Pb). J Mol Catal A Chem 233:133–139